Field trip 5

Rockfall-triggered, long-runout ‚two-layer scree/snow avalanche', old rock avalanche deposit, and epigenetic canyon incision (Northern Calcareous Alps): consequences for hazard assessment and landscape history

Diethard Sanders[1], Alexander Preh[2], Thomas Sausgruber[3], Hannah Pomella[1], Marc Ostermann[1], Andrea Sedlmaier[1]

[1] Institute of Geology, University of Innsbruck, A-6020 Innsbruck, Austria/EU;
e-mail: Diethard.Sanders@uibk.ac.at;
Hannah.Pomella@uibk.ac.at; Marc.Ostermann@uibk.ac.at

[2] Institute of Geotechnics, Vienna University of Technology, A-1040 Vienna; Austria/EU;
e-mail: alexander.preh@tuwien.ac.at

[3] Austrian Service for Torrent and Avalanche Control, A-6020 Innsbruck, Austria/EU;
e-mail: thomas.sausgruber@die-wildbach.at

1 Introduction

Snow avalanches are a major hazard in populated mountain ranges. Relative to most other geomaterials, the physical properties of snow vary over an extremely wide range and may change within days to hours. The capacity of avalanches to transport foreign materials (e.g., trees, rock fragments, soil) strongly depends on kinetic energy and mode of avalanche propagation as a function of snow type. Ground-hugging avalanches of coarse-granular snow typically are efficient in uprooting or truncating forest, rip-up of soil, and transportation of scree. Most research on erosion and transportation of foreign materials is focused on ground avalanches that develop by gravitational instability of the snow cover itself.

Another, more rare type of avalanche is kicked off by rockfall impact. As demonstrated on the excursion, large rockfalls hitting snow-covered slopes may develop a specific avalanche type in which the scree is carried piggyback on top of pure sliding snow; the resulting ‚two-layer scree/snow avalanches' can copiously carry clasts up to boulder size, and show exceptionally long runout (Figs. 1, 2). This type of avalanche not only is pertinent for hazard assessment, but may significantly contribute to shaping of periglacial landforms and deposits. With a volume of 75.000 cbm, the rockfall deposit seen on the excursion is near the 100.000-cbm limit suggested to separate rockfalls from rock avalances (Evans et al., 2006).

Over the past 15 years or so, a growing awareness of rock avalanches *s. str*. descended on ice or snow is related to increased airbourne observation, and by trigger events such as the 2008 M8 Denali earthquake. Such rock avalanches show features that may allow their identification also if the ice or snow has long disappeared. In the western Northern Calcareous Alps a number of mass flows was identified and mapped in LIDAR topography that most probably descended in association with snow or ice (**Sanders et al., 2016**). In the excursion area, a rock avalanche deposit is present that – except for geological mapping well-ago (**Ampferer and Ohnesorge, 1912**) – was hitherto overgone. Field mapping in LIDAR topography revealed that this rock avalanche was highly mobile and shows some characteristics suggestive of runout on snow (**Fig. 1**). By blocking the pre-glacial trunk valley off drainage, the rock avalanche further enforced the incision of an epigenetic bedrock canyon (**Sanders, 2015**); the hydrological and geomorphological impacts of that event thus coin the entire area NW of Telfs township till today.

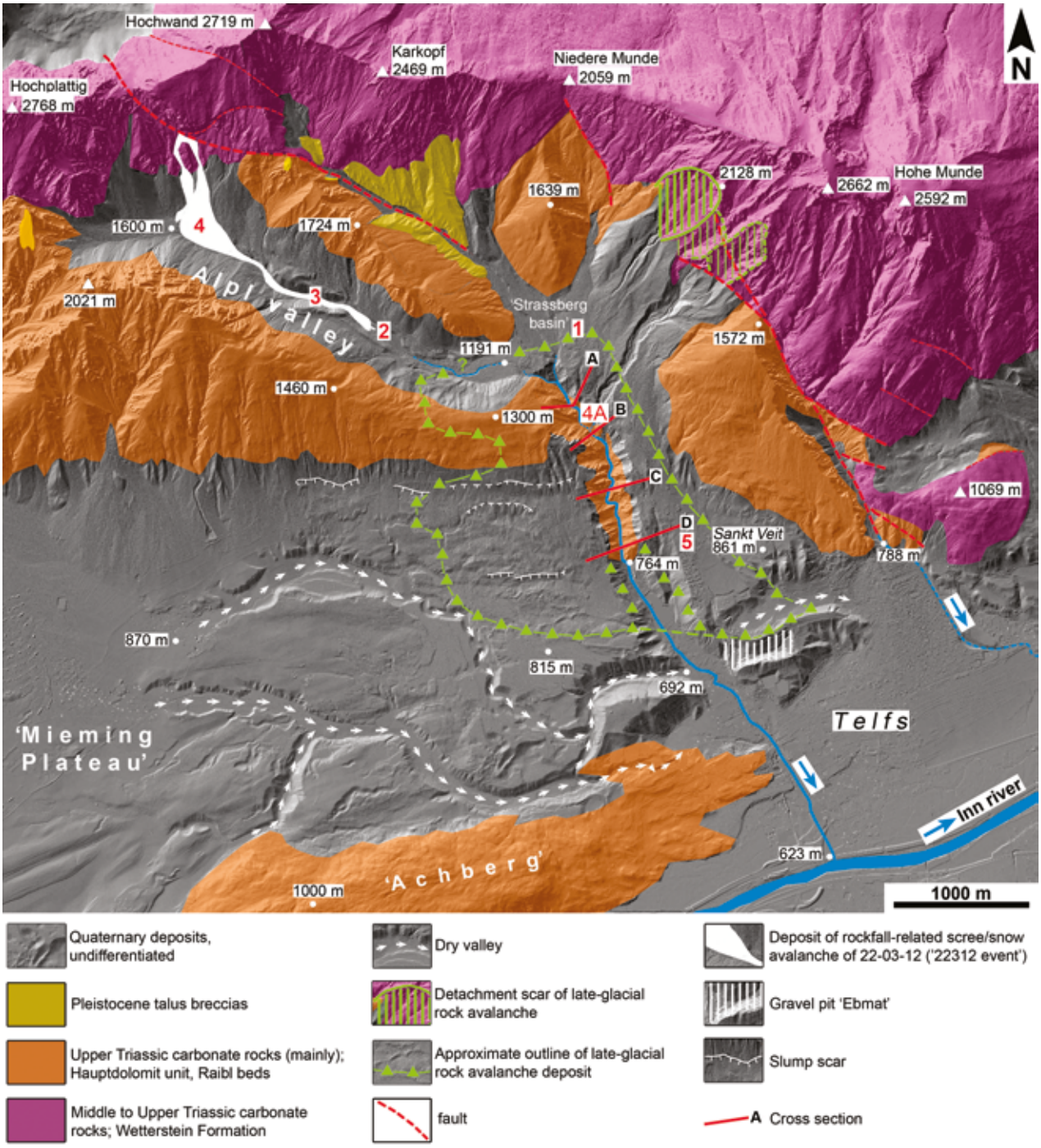

Fig. 1: Geological overview of excursion area. Stops 1 to 5 are labeled with red numbers. Note: (1) depositional area (white) of scree/snow avalanche induced by 75.000-cbm rockfall on March 22nd, 2012 (‚22312 event'); (2) deposit of ~11 Mm^3 post-glacial rock avalanche outlined by green triangles; (3) the bedrock gorge of Strassberg valley. Red lines labeled A to D denote traces of cross-sections shown in **Fig. 10**.

2 Setting

The excursion area is located near the southern margin of the Northern Calcareous Alps (NCA), a stack of thrust nappes dominated by Triassic shallow-water carbonate rocks (**Tollmann, 1976**). The area of interest is part of the ‚Inntal' thrust nappe that here comprises three stratigraphic units, each characterized by rock types well-identifiable in the field (Fig. 1**)**. Of the three units,

it is mainly the limestone succession of the thick, competent Wetterstein Formation (Middle to Upper Triassic *pro parte*) that supports the highest cliffs and summits. In the central and southern part of the considered area, more gently-shaped crests and ridges are underlain by the dolostone succession of the Hauptdolomit unit (Upper Triassic *pro parte*). During Alpine deformation, the dolostones of the Hauptdolomit reacted brittlely and were subject to dense jointing and faulting; this results in comparatively high erobadility of this unit. The Triassic succession is dismembered by a system of NW-trending faults (Fig. 1). Stratigraphic offset and fault displacement indicators mainly indicate dextral strike-slip and normal faulting. This ‚Telfs fault system' developed in reaction to NW-ward thrusting of a basement block a few kilometers farther toward the South. The Telfs fault system, or a precursor to it, may be active since the Neogene. The main valleys of the excursion area all show the same trends as those of the younger faults of the system. The fault system still is active, as suggested by abundant macro-seismic events.

In the Eastern Alps, four full glacials are distinguished (**van Husen and Reitner, 2011**). In intramontane settings, the last glacial maximum (LGM) is recorded mainly by proglacial fluvio-lacustrine successions and by basal till. The post-LGM warming was punctuated by stadials, i.e. by phases of climatic cooling and glacial re-advance, as recorded chiefly by glacial moraines (**Penck and Brückner, 1909; Reitner, 2007**). In addition, in particular in the NCA, sediment bodies of alluvial and hillslope origin that accumulated under deglacial to paraglacial conditions comprise significant volumes and landscape elements (**Sanders & Ostermann, 2011; Sanders, 2012**).

In the excursion area, the oldest Quaternary deposits comprise large erosional remnants of talus breccias. Most of the breccias onlap rock cliffs, but some are preserved as ‚perched' erosional relicts isolated from their present geomorphic setting. The talus breccias show features of syn- to post-depositional deformation, including: (1) monoclines and recumbent folds, (2) drag along the contact to the Triassic rock substrate, (3) clasts up to boulder size that were fractured while embedded in the breccia, and (4) stratal packages tilted against paleoslope. The age of the breccias is unknown, except that they predate the LGM. In its topographically lower part, the excursion area is characterized by a succession of proglacial outwash ahead of the advancing LGM Inn ice stream, interfingering with local-supplied aggrading alluvial fans; these, in turn, are overlain, by basal till of the LGM. **Poscher (1993)** identified a proglacial aggrading alluvial fan or braid delta supplied from Straßberg valley, and that prograded into a proglacial lake. This delta aggraded to a level at least as high as the present upper brink of the lower reach of Strassberg bedrock gorge. The delta, however, was not supplied from the presently active canyon, but from a pre-LGM precursor of Strassberg valley that is filled with proglacial sediments and rock avalanche deposits til today. During the LGM, most of the area was buried under ice. Transfluence of peak glacial ice across the southern crest of Alpl valley is indicated by clasts of metamorphic rocks up to near the valley head.

In Alpl valley, post-LGM moraines and relicts of debris-rich glaciers were assigned by **Senarclens-Grancy (1938**) to stadial advances (Fig. 2). Other significant post-LGM depositional systems include scree slopes and alluvial fans. The present upper treeline in the area is mainly controlled by distribution of rocky slopes, and by scree slope activity. A few areas higher than ~1700-1800 m a.s.l. are covered by dwarf pines. Actively aggrading scree slopes are largely confined to altitudes >1600 m a.s.l. in the proximal part of Alpl valley. Most of the present geomorphic activity in the area is confined to rockfall- and offwash-related sediment supply from cliffs down to scree slopes. In addition, snow avalanches transport scree up to boulder-size grade down along talus and valley bottoms.

In the overview map the extent of the old, presumably late-glacial/deglacial rock avalanche deposit as well as of the 22312-avalanche are indicated (Fig. 1). **Ampferer & Ohnesorge (1912**) were the last who mapped the rock avalanche deposit, and interpreted it as a late-glacial ‚blocky till' (qm_3 in their map legend). Since then, it fell forgotten. Relative to similar valleys in the NCA, the entire area shows an atypical morphology. First, it is unusual that a valley the width and length of Strassberg rakes down with a bedrock canyon whereas

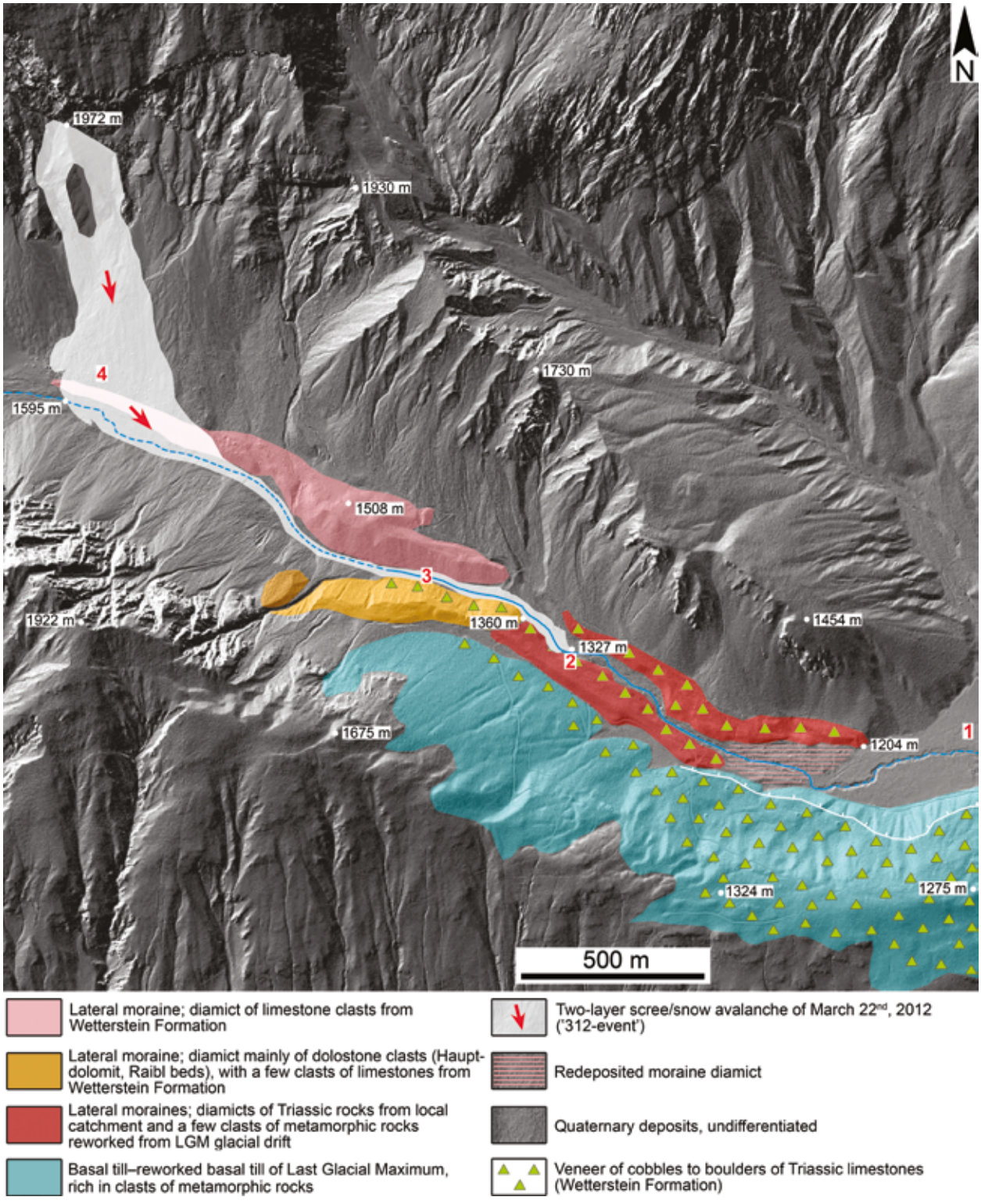

Fig. 2: Map showing selected Quaternary deposits along Alpl valley. The right valley flank is covered by basal till–redeposited basal till of the Last Glacial Maximum. The valley thalweg is flanked by extremely poorly-sorted, bouldery diamicts that are interpreted as lateral moraines of late-glacial ice tongues. The right valley flank and the moraines in the lower part of Alpl valley are veneered by bouldery scree composed only of Wetterstein limestone (=rock-avalanche deposit); this scree is derived from the high cliff of Hohe Munde along the eastern side of the Strassberg intramontane basin (cf. Fig. 1). Depositional area of 22312-event shown in white. Red numbers indicate excusion stops.

the adjacent, wider former valley still is filled with Quaternary deposits; second, the bedrock canyon tapers out upstream within the rock avalanche deposit, and the entire upper part of the catchment (Strassberg basin, Hintereggen valley, Alpl valley) is graded to an elevated base-level placed by the rock-avalanche deposit (Figs. 1, 2). This indicates that the entire catchment was strongly disturbed by rock avalanche deposition, to a degree that it is still far from geomorphic equilibrium (**Sanders, 2015**).

Fig. 3: Satellite orthoimage showing depositional area of the 22312-scree/snow avalanche.

3 22312-rockfall and two-layer avalanche

3.1 The event

The rockfall detached a few minutes before midnight of March 22nd, 2012 from the south-facing cliff of mount Hochwand. At least the majority of the rock mass collapsed at once, as indicated by a seismic event of M=1.4 recorded by the Central Institute of Meteorology and Geodynamics Austria in Vienna (**Preh & Sausgruber, 2015**). Rock detachment took place along, both, vertically-tilted bedding planes and sets of subvertical fault planes parallel and oblique to the cliff surface; the fault planes fit with the Telfs fault system (cf. Fig. 1, Fig. 3). In the avalanche deposit, many boulders are bounded along one or several of their surface facets by fault planes. The detached rock mass had the shape of a thin slice approximately 240 meters in height (Fig. 4A).

The rock mass first slid down a very steep ‚rock ramp' before hitting two triangular slope facets (cf. Fig. 1). Along the toe of the cliff and on the overridden areas of the slope facets the snow cover, scree, vegetation of dwarf pine and soil were all ripped off by rockfall impact (Fig. 4A). From the impact area, the disintegrated rock mass rushed onto a scree slope that was covered with a layer ~1-2 meters in thickness of coarse-granular snow (**Preh & Sausgruber, 2015**). On the talus apron some 200-250 meters downslope of the lower fringe of the impact area, a two-layer scree/snow avalanche deposit was identified by field inspection; this indicates very proximal and effective development of this type of avalanche by frontal entrainment of snow. On the wide scree apron below mount Hochwand, the two-layer avalanche opened to a maximum width of ~300 m while flowing down (Fig. 3). In this stage, the rockfall material that rode on the avalanche snow comprised no more than a veneer up to a few decimeters in thickness, scattered with many projecting boulders (Fig. 4B).

Along the toe of the scree slope, the avalanche passed over a steep (~35-45°) step vegetated by dwarf pine; the step is between 5-15 m in height, and represents a lateral moraine of a late-glacial ice tongue (Fig. 2, Fig. 4C). Along this step, it is observed that some parts of the two-layer avalanche overrode it without damage to vegetation and soil; in other sectors, dwarf pine stands are heavily scratched or torn off, and soil was ripped up (Fig. 4C). We assume that these differences in vegetation damage and soil erosion result from thinning of the snowflow over the step: where no large boulders were present in the snowflow, the thinned flow by-passed the step without erosion; where large boulders were present, the flow thinning grounded the boulders while riding down.

After passage of‚The Step', the avalanche took the last turn to the thalweg of Alpl valley. The radius of that turn was used to calculate avalanche velocity. The radii of the turns were used to calculate avalanche velocities (Tab. 1). When the snow/rock mass poured into the inner, relatively narrow and steeper part of Alpl valley, it re-accelerated, and from there ran out for some 2 kilometers along the valley. A most distinctive feature of the two-layer avalanche thus is its exceptionally long run-out, relative to a potential rockfall of the same volume onto a land surface devoid of snow (**Preh & Sausgruber, 2015**).

3.2 Key parameters and back analysis

The runout of 2.6 km of the two-layer rock/snow avalanche corresponds to an angle of reach (fahrböschung) of 17.8°. This is an exceptionally low angle that, however, is still within the lower fringe of fahrböschung values observed for rock avalanches (cf. **Collins & Melosh, 2003**). Assuming a conservative average thickness of 2 m of the final avalanche deposit immediately after the event, i. e., rockfall scree plus snow, yields a minimum volume of 500.000 cbm; this indicates that the volume of the‚fresh' avalanche deposit consisted to roughly a 6 times more of entrained snow than the 75.000 cbm of rockfall material (**Preh & Sausgruber, 2015**).

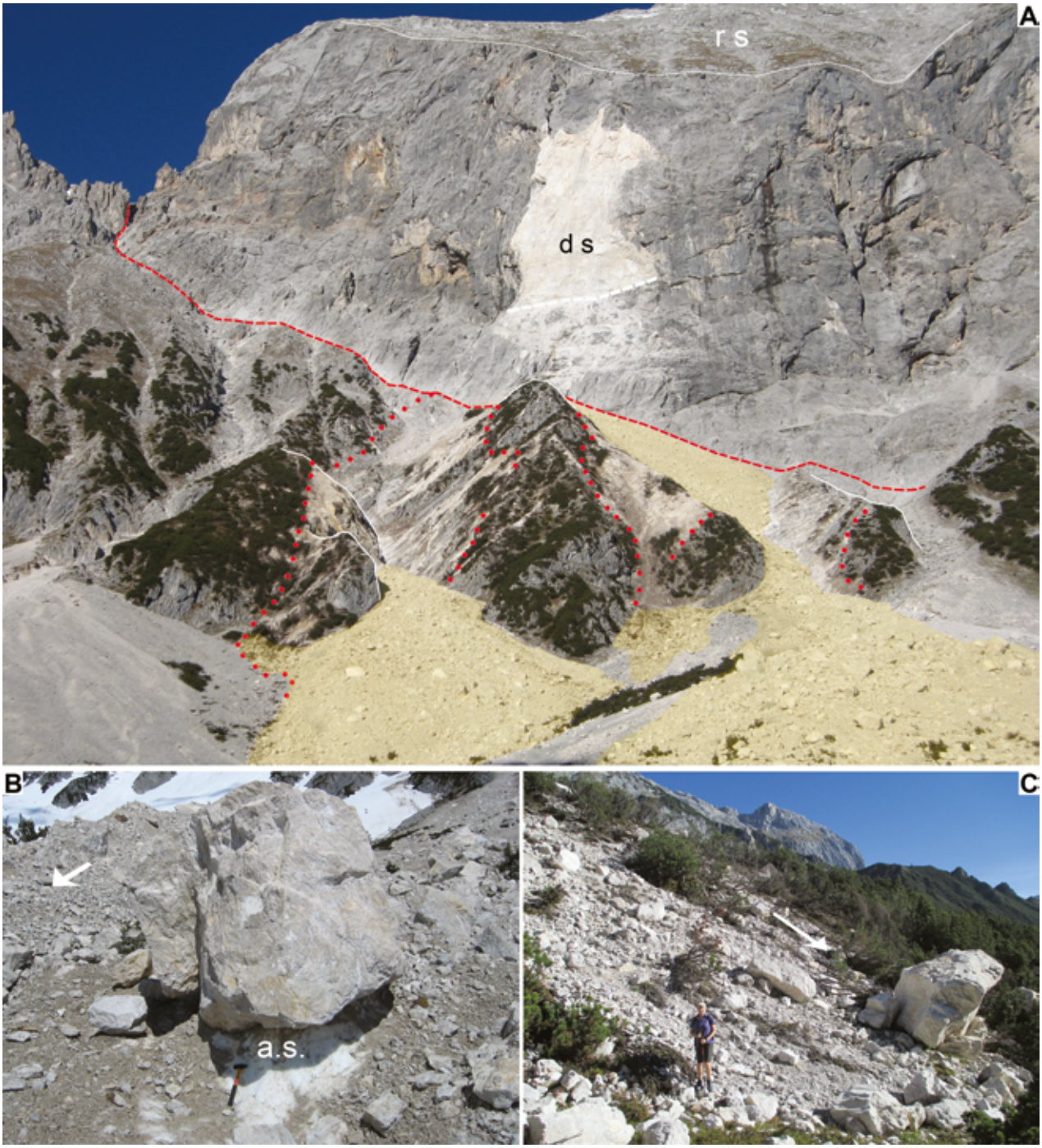

Fig. 4: **A**) In its upper part, the southern face of mount Hohe Wand (cf. Fig. 1) shows a large relict of a graded rock slope (rs); downslope, it sharply knicks off into a subvertical cliff. The strike of the cliff is controlled by erosion along a NW-SE striking fault (indicated by red dashed line; see also Fig. 1) that fits with the Telfs fault system (see text). The detachment scar (ds) of the 75.000-cbm rockfall is 230 m in vertical height. The lower tip line of rock defacement is indicated by white dashes. After hitting a snow-covered rocky slope facet along the toe of the cliff, the rockfall mass parted into two branches that each rushed out along a scree-veneered chute between rocky slope facets. On the slope facets, areas exposed to the full brunt of the downrushing mixture of rockfall scree and snow were ripped of vegetation of dwarf pine and soil (areas outlined by red dots); areas in the flow lee, in turn, did not suffer significant erosion. The final deposit of the 22312-rockfall event (area labeled with light yellow hue), shown after compelte melting of avalanche snow, is an unsorted veneer with boulders up to more than 10 m in size. **B**) Deposit of two-layer scree/snow avalanche, April 2012, on the talus approximately 500 meters downslope of the rockfall impact area. The entire rockfall-derived scree, including the boulder in foreground, was kept afloat on a lower, thicker layer of pure avalanche snow (a.s.) entrained into the propagating flow. White arrow denotes flow direction. Hammer is 35 cm in length. **C**) Avalanche deposit on ‚The Step' (= a steep flank of an older lateral moraine, cf. Fig. 2) after snowmelt. White arrow denotes flow direction. Person for scale.

The avalanche was back-analyzed using the continuum mechanics numerical code DAN3D (**McDougall & Hungr, 2004**). DAN3D uses a semi-empirical approach based on the concept of "equivalent fluid", defined by **Hungr (1995**). In this framework, the heterogeneous and complex landslide material is modelled as a hypothetical material, which is governed by simple internal and basal rheological relationships that may be different from each other. The internal rheology is assumed to be frictional and is governed by only one parameter, the internal friction angle. The shear resistance at the base of the flow is modelled by means of an open rheological kernel, which allows the use of frictional (with constant pore-pressure ratio), plastic, Bingham, Voellmy and other rheologies. DAN3D and the Voellmy model produced the best results coinciding with reality. The best results in terms of travel distance and duration and spatial distribution of velocities and flow/deposit depths is obtained using a friction coefficient f of 0.1 and a turbulence coefficient ξ of 500 m/s^2.

Fig. 5 shows the debris distribution and impacted area calculated by means of DAN3D. The simulated impacted area agrees fairly well with the mapped outer margins of the avalanche deposits (yellow dots shown in Fig. 5). The majority of the rock debris (Fig. 5) has been accumulated in the simulation below the elevation line of 1,600 m. This is in conflict with the observations, where the deposits are distributed along the entire runout path. A plot of the maximum simulated flow velocities recorded along the path is shown in Fig. 6. The highest velocities, up to about 52 m/s, were recorded at the uppermost part of the talus slope between the toe of the rock cliff (detachment zone) and the outcropping bedrock. The model shows a significant drop of the flow

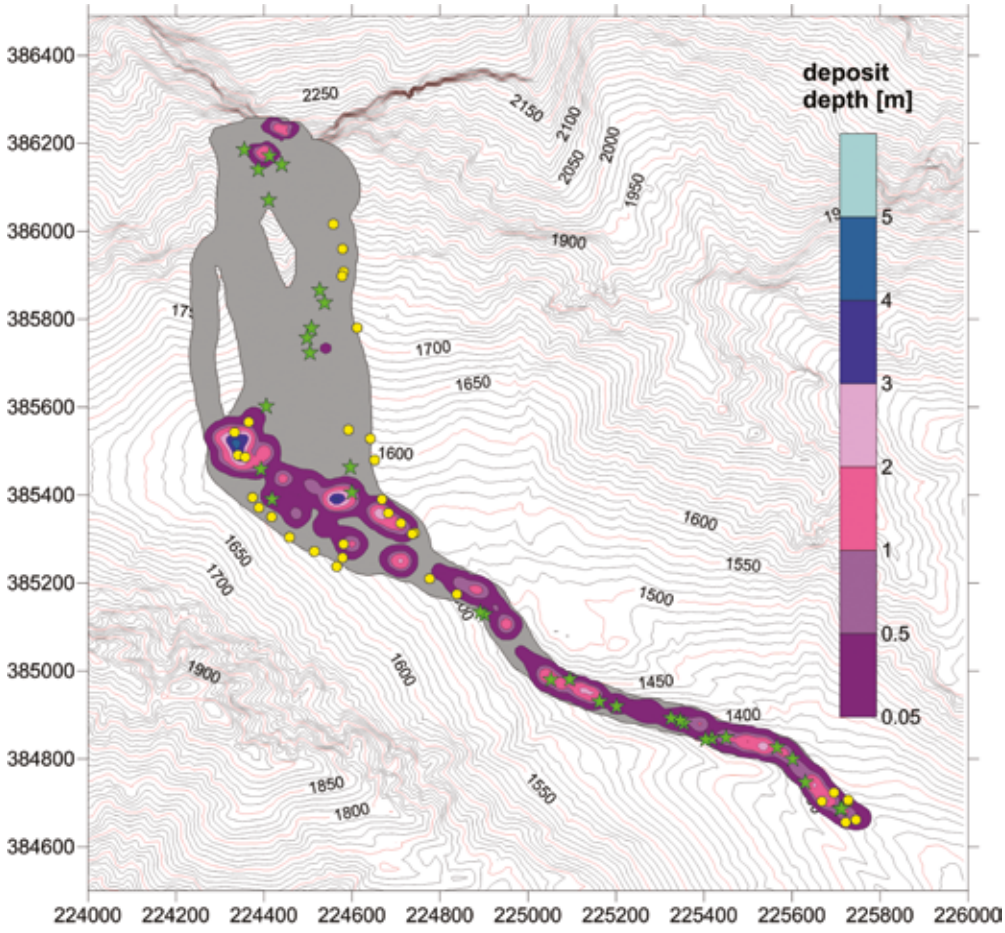

Fig. 5: Plot of simulated deposit distribution (10-m isohypse contours). The grey shade indicates the area of the rock-snow avalanche. Yellow dots mark the outer margins of the rock-snow avalanche; green stars are locations of big boulders and significant points along the path (**Preh & Sausgruber, 2016**).

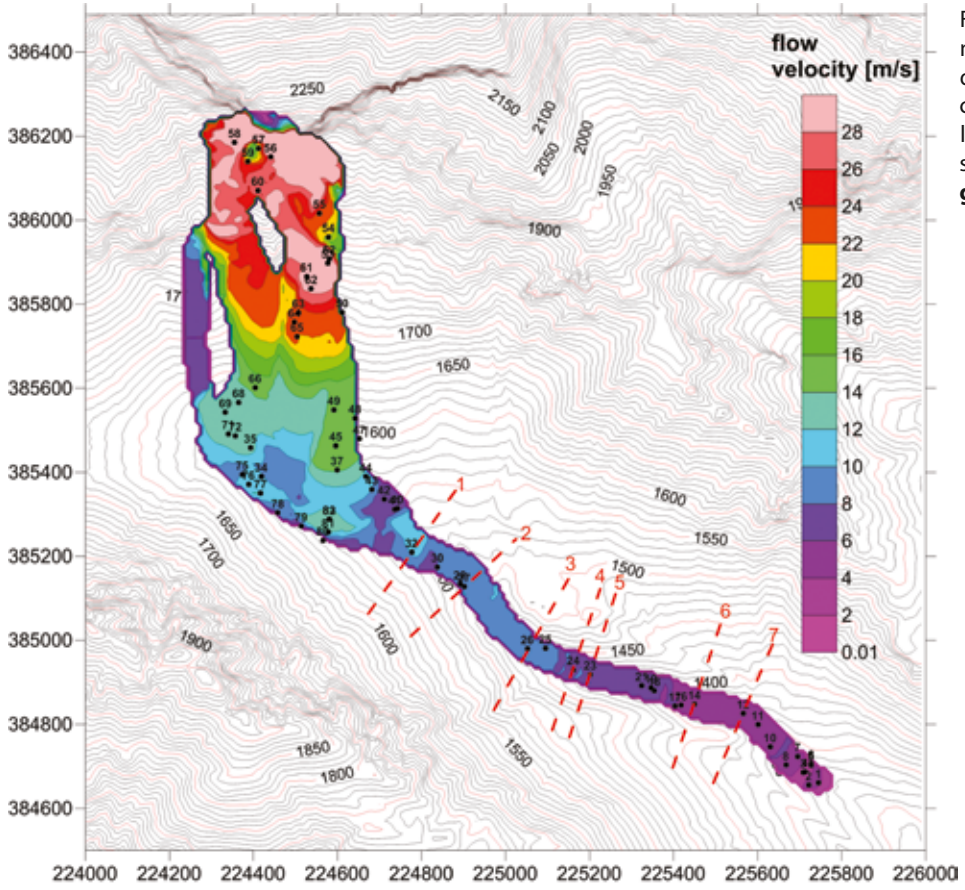

Fig. 6: Plot of maximum simulated flow velocities. The dashed lines mark seven cross sections used for velocity estimation based on superelevation (**Preh & Sausgruber, 2016**).

	Flow velocities (m/s) estimated based on superelevation		Flow velocities (m/s) calculated by DAN3D
Section No	Hungr	Spreafico	
1	7.2	8.7	9.4
2	8.1	10.0	9.6
3	9.4	11.4	9.1
4	11.8	10.4	8.5
5	10.6	13.0	7.7
6	8.5	10.5	5.6
7	5.3	6.6	5.9
Average	8.7	10.1	8.0

Table 1: Comparison of max. flow velocities estimated based on superelevation (after Hungr et al. 1984 and Spreafico et al. 1996) and calculated by the DAN3D-code (Preh & Sausgruber, 2016).

velocity in the 80° bend at the toe of the talus. Afterwards the simulated avalanche flowed the 9.4° inclined and tight shaped valley floor downwards with a relatively slow average velocity of 8 m/s. The dashed lines in Fig. 6 represent the locations of seven cross sections used for velocity estimation based on superelevation. A comparison of superelevation-based (after **Hungr et al., 1984, and Spreafico et al., 1996**) and simulated velocities is given in Table 1. The back-calculated flow velocities suggest that the entire event spanned some five minutes (300 s) in duration.

3.3 Rock/snow avalanche deposit

3.3.1 Surface features

At surface, laterally alongside the cover of rockfall-related materials, the avalanche was fringed by a mass of more-or-less pure chunks and balls of snow, as typical for avalanches of coarse-granular snow. On the Hochwand scree apron, the scree-covered part of the rock/snow avalanche showed an irregular surface with gentle downslope-elongated ridges and grooves; otherwise, no clear-cut differentiation of surface features on the fresh avalanche deposit could be identified.
Along most of its runout in Alpl valley, the avalanche was flanked by a fringe up to a few meters in width of more-or-less pure avalanche snow (Fig. 7).

Similarly, the snout of the avalanche showed as a pile of chunks and balls of pure snow. Along Alpl valley, in cross-section, the top of the fresh avalanche deposit became progressively more rich in rockfall-derived material from the lateral margins inward to the thalweg of the snowflow. At several positions along the deposit, an outer and an inner ‚flow tongue', respectively, could be distinguished by the foreign materials carried on top of flow (rockfall material only; or: rockfall material + soil + uprooted dwarf pines). The outer flow tongue in many cases clearly ran in a higher, elevated position relative to the inner flow tongue. The inner flow tongue was sharply separated along slide planes of ice (see below for description) from the higher-topped outer one (Fig. 7).

The snout of the avalanche was a pile a few meters to some 10 m in thickness of pure snow (Fig. 8A); only on top of the snow pile, a few meters upstream of the pile's brink, unsorted rockfall sediment of clay- to boulder-size grade started as scattered patches. A short distance farther upstream, the entire top of the avalanche was coated with unsorted rockfall material (Fig. 8B, 8C). The terminus of the avalanche was differentiated into three snowflow tongues (Fig. 8E). The highest, central snowflow tongue was c. 10 m in height.

3.3.2 Features in vertical section

From the Hochwand scree apron down to the snout of the snowflow, in vertical section, the avalanche snow displayed: (a) thin slide planes, preserved as laminae of transparent ice; these slide planes were subparallel to the local avalanche surface, and showed a typical vertical spacing of a few decimeters to a few meters (Fig. 8A); (b) locally, deeper within the avalanche deposit, a parallel lamination of the avalanche snow intercalated between the slide planes (Fig. 8D). Slide planes were sculpted with parallel ‚grooves' similar to corrugations on brittle fault planes (Fig. 7).
The main loci where uprooting of dwarf pines as well as rip-up of soil and scree took place include: (a) the rockfall impact area, (b) the very steep slope of ‚The Step', and (c) elongate scars along the left side of Alpl valley, where the avalanche was forced to curve. At all other locations, including most of the Hochwand scree apron, no evidence for ground erosion was observed along the avalanche track.

3.3.3 Sediment

Over the entire distance from the scree apron to the snout of the avalanche deposit, the two-layer separation into rockfall scree floating on avalanche snow underneath was conserved; similarly, over the entire extent of the avalanche, there was no evidence for sorting or grain-size segregation, and the rockfall-derived sediment contained the full spectrum from clay- to boulder size grade. After complete meltdown of snow, the clay- to cobble-sized clastic material comprised a patchy veneer up to a few decimeters in thickness at most. With time, this veneer will be reworked to unidentifiability with respect to its origin, and only the boulder litter will remain as a record of event deposition.
In the sediment fraction ≤16 mm grain size, the percentage of sand plus ‚mud' (=grains < 0.063 mm in size) of eleven (11) wet-sieved samples ranges from 9.73 – 13.61 – 17.7 weight percent. The fraction of ‚mud' < 0.063 mm of eleven samples ranges from 2.5 – 3.1 – 4.3 weight percent. Despite the relatively low content of sand and mud in the size fraction up to 16 mm, it sufficed to impart a distinct cohesiveness and ‚muddy appearance on touch' to this comparatively fine-grained sediment fraction. Electron microscopic investigation shows that that fine-grained matrix of the rockfall consists of angular mineral fragments down to submicron size (**Flatscher, 2014; Prendl, 2015**).

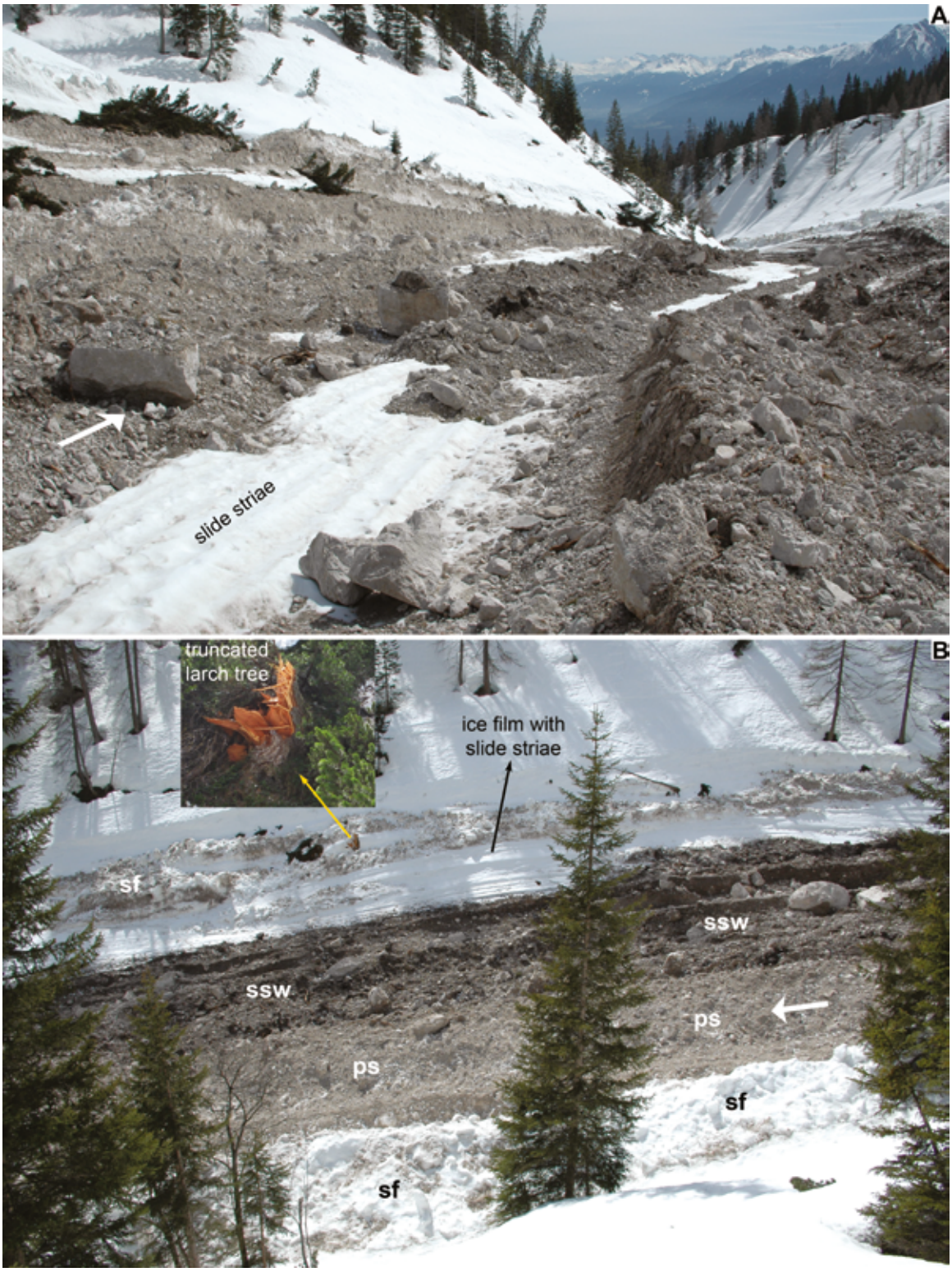

Fig. 7: **A**) April 2012. Downflow view (white arrow) from c. 1530 m asl along 22312-avalanche deposit. Note outward-to-inward partitioning of deposit into discrete flow tongues. The flow tongues are laterally separated from each other by a steep morphological step (red arrowtips) associated with alongflow shear planes in snow. **B**) April 2012. View to south across 22312-avalanche deposit at c. 1390 m asl; white arrow shows flow direction. Across the rock/snow avalanche deposit, a typical partitioning is seen. The highest and outermost part is a fringe of pure to slightly scree-littered avalanche snow (snow fringe, sf). At many locations along the fresh deposit, this snow fringe was visibly underlain by a thin plane of ice sculpted with slide striae (similar to corrugations on fault planes). From the snow fringe inward toward the flow center, the deposit was partitioned into discrete tongues laterally separated by flow-parallel shear planes within avalanche snow. In the photo, the inner part of the flow was partitioned into a tongue characterized by pure rockfall-derived scree (ps), sharply separated from an adjacent flow tongue carrying a mixture of rockfall scree, soil and wood (dwarf pines) (ssw). Near the outermost right margin of the snowflow, a larch c. 35 cm diameter was sharply truncated.

Fig. 8: **A**) April 2012. Central terminal snout of 22312-rock/snow avalanche. Scree littered piggyback on pure avalanche snow started only some 10–15 meters upstream of the distal tip of the snowflow deposit. Shear plane within avalanche snow indicated by black arrows. Person for scale. **B**) September 2012. Detail of terminal part of 22312-event deposit, after complete melting of avalanche snow. Patch of broken and truncated spruce (see Fig. 8E for location). When the spruce were broken off, the avalanche was roughly some 8-10 m in height; the bouldery veneer was laid down along the knicked base of the trees only after meltdown of snow (i. e., the trees were truncated by snowflow, not by the moving boulders). **C**) September 2012. View downflow towards the terminus of 22312-scree deposit, showing boulders littered on ground. Note truncated spruce (white arrow), but growth of shrubs and herbs from undamaged soil cover underneath the bouldery scree veneer. **D**) Mai 2012. Meltdown of 22312-avalanche snow reveals sets of shear planes of ice (indicated by black arrows) that are subparallel to ground surface and to each other. **E**) Satellite image of terminal part of 22312-two layer scree/snow avalanche, after complete snowmelt. Note: (1) differentation of flow terminus into three snouts (labeled 1 to 3), and (2) small patch of spruce stand spared from truncation, between flow snout 2 and 3. Larger boulders highlighted as black patches.

4 Rock avalanche deposit

The rock avalanche detached from the high western slopes of mount Hohe Munde. This is indicated by: (a) presence of a distinct lunate scar in the western cliff, (b) composition of the RAD practically exclusively of clasts from the Wetterstein Formation, and (c) the runout path of the rock avalanche (Fig. 1, Fig. 9A).
Evidence suggestive of a relatively high postglacial age of the event includes: (i) in its left-side proximal to medial part, the RAD is partly buried by younger slope- and alluvial-fan deposits that, today, all are inactive (Fig. 9B); (ii) the rock avalanche does not fill the former Strassberg valley, but instead comprises a veneer to gently ? incised chute above LGM basal till and/or LGM proglacial-fluvial deposits; and (iii) radiocarbon ages of up to 11180-11170 cal BP from soils above the RAD (Fig. 9B, 9C) (**Sanders, 2015**).

Because of a relatively long duration of erosional overprint of potential detachment scars in the western cliff of Hohe Munde, several solutions for differential rock volumes were calculated; the most probable solution that is also associated with the most obvious scar is 11 Mm^3. Adding other, smaller scars in the cliff, a maximum total volume of 19 Mm^3 resulted. With a fahrböschung angle α of 16° and a probable volume V of 11 Mm^3, the rock avalanche deposit is the range of typical V/α ratios of other catastrophic slope failures (cf. **Collins & Melosh, 2003**).
After detachment, the rock mass ran down the western slope of Hohe Munde into Strassberg valley. At the valley floor, part of the avalanche completely blocked the pre-LGM valley; this set the base-level for the Strassberg intramontane basin, and precluded the re-incision of the trunk stream into the proglacial Quaternary valley filling (Fig. 1, Fig. 10). A part of the avalanche ran up onto the opposite rock slope and crest (= right flank of Alpl valley) over considerable distance; this testifies to a high mobility and high velocity of the avalanche (Fig. 1). It seems even possible that the frontal part of the rock avalanche traversed the mountain crest, and from there re-accelerated over a very steep rocky slope onto the Mieming Plateau farther down, where it might have merged with other parts of the propagating avalanche. Notably, on the overrun rock slope and crest, the RAD comprises a thin veneer that might go unrecognized if it were not for the litter of boulders of Wetterstein Limestone.
That branch of the avalanche that propagated more directly out along Strassberg valley spread laterally over the wide, gently sloping Mieming Plateau. In the distalmost western part of the RAD, flow lines still are evident in LIDAR. As mentioned, closely east of the exit of Strassberg gorge, the bedrock disappears, and the former valley still is filled to the brim with proglacial fluvio-lacustrine deposits and LGM basal till. This indicates that the former Strassberg valley was not nearly cleared of sediment when the rock avalanche descended.

In a few deeper exposures in the proximal part, the RAD shows a densely-packed, clast-supported fabric composed of angular to rounded cataclasts of Wetterstein limestone (Fig. 9D, 9E). Such fabrics typically contain a matrix of cataclastic gouge (Fig. 9E). A most notable aspect of the RAD is its low thickness over large areas. Where the RAD fills the former upper reach of the pre-LGM Strassberg valley, it is up to c. 60-70 m in thickness. This may indicate limited fluvial re-incision along the original (pre-LGM) valley thalweg but similarly, or in addition, may result from erosion along the base of the rock avalanche that is quenched into the valley (= is forced to sharply change direction, so exerts much more kinetic energy into basal and internal friction). Farther downslope, in the area of Sonnenberg, the left (eastern) side of the RAD is a few meters in thickness at least; field mapping suggests that the deposit may be some 10-15 m in thickness (Fig. 9C).

Over the wide western part of the RAD, in contrast, many outcrops indicate a low thickness down to a few decimeters, yet the area is littered with boulders up to ~20 m in size. In this area, however, the RAD and part of the underlying till are involved in slumping, so part of the thinning may result from extension in slumps. Nevertheless, also in areas not affected by slumping, the RAD seems to attain a thickness of a few meters at most. As mentioned, on the mountain ridge ran up by the rock avalanche, it is the boulder litter rather than the low thickness and patchiness of the deposit that highlights avalanche transport.

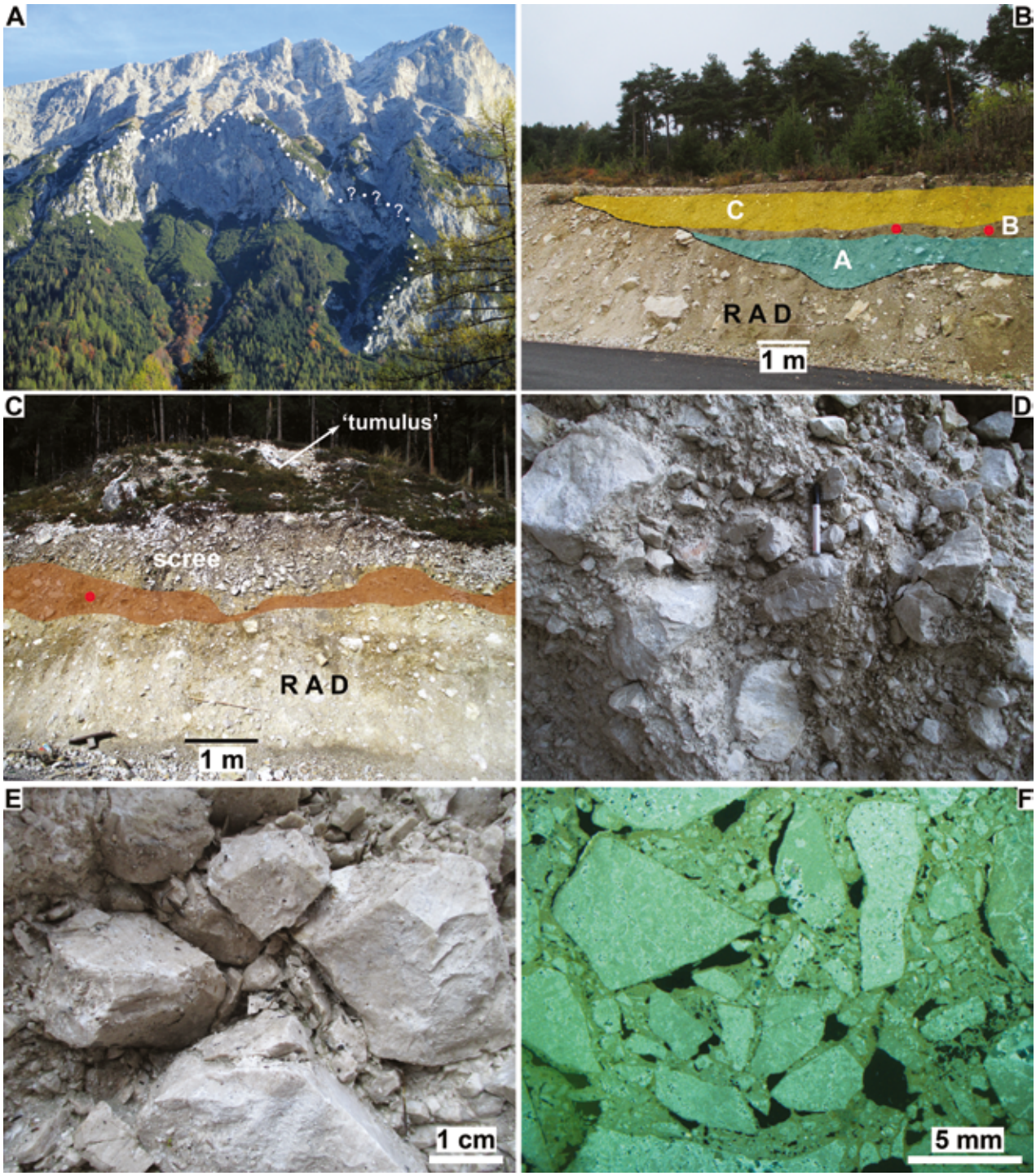

Fig. 9: **A**) Western cliffs of mount Hohe Munde, with detachment scar of 11 Mm^3 rock outlined by white dots. **B**) Distal part of rock avalanche deposit (RAD), overlain by: (A) cohesive debris-flow deposit rich in clasts of metamorphic rocks (including striated clasts) and with a few clasts derived from the local rock substrate; (B) level of sandy soil; (C) faintly stratified package of sheet-flow deposits of angular to subrounded, fine- to medium-pebbly scree derived from the local rock substrate (NCA), and with rare clasts of metamorphic rocks. Unit C is toped by actual soil. Red dots mark position of radiocarbon samples. **C**) Distal part of rock avalanche deposit (RAD), overlain by sandy soil mixed with angular scree of Wetterstein limestone (brown level). The soil-rich level, in turn, is overlain by a scree halo accumulated by physical degradation of a once higher rock-avalanche boulder of Wetterstein limestone to a relictic hummock (‚tumulus'). Red dot denotes location of radiocarbon sample. **D**) Exposure of rock avalanche an estimated 30-40 meters below former top of deposit. The rock avalanche mass consists of angular to subrounded clasts exclusively of Wetterstein limestone. The clasts are densely packed into a disordered fabric; a few of the larger clasts are fractured in situ. Pen is 14 cm long. **E**) Detail of same outcrop as in preceeding figure. The interstitial space between larger clasts is filled with very angular rock chips‚splintered off' the larger clasts and/or derived from complete in-situ fragmentation of smaller clasts. **F**) Thin section of outcrop shown in **Fig. 9D**. Clast-supported fabric with lithified matrix of cataclastic gouge. Note pores (black patches) produced by eluviation/dissolution of gouge. Crossed nicols.

Together, the evidence suggests that part of the rock avalanche propagated on a cover of snow. The run-up onto the opposite mountain slope as a thin, patchy veneer of rock fragments up to boulder size is mechanically impossible; a carrier substrate is required that, under the given circumstances, was provided by snow (not dead ice). Whereas this run-up requires high velocity, in the lower western part of the rock avalanche, velocities not necessarily were high. If a substrate of snow was present, the avalanche may have propagated with a few meters per seconds or even slower over a long distance, provided that mechanical coupling to a gravitationally unstable upper part of the avalanche mass was upheld. This is underscored by the calculated velocity curve of the 1987-Bormio rockslide (**Crosta et al., 2004**).

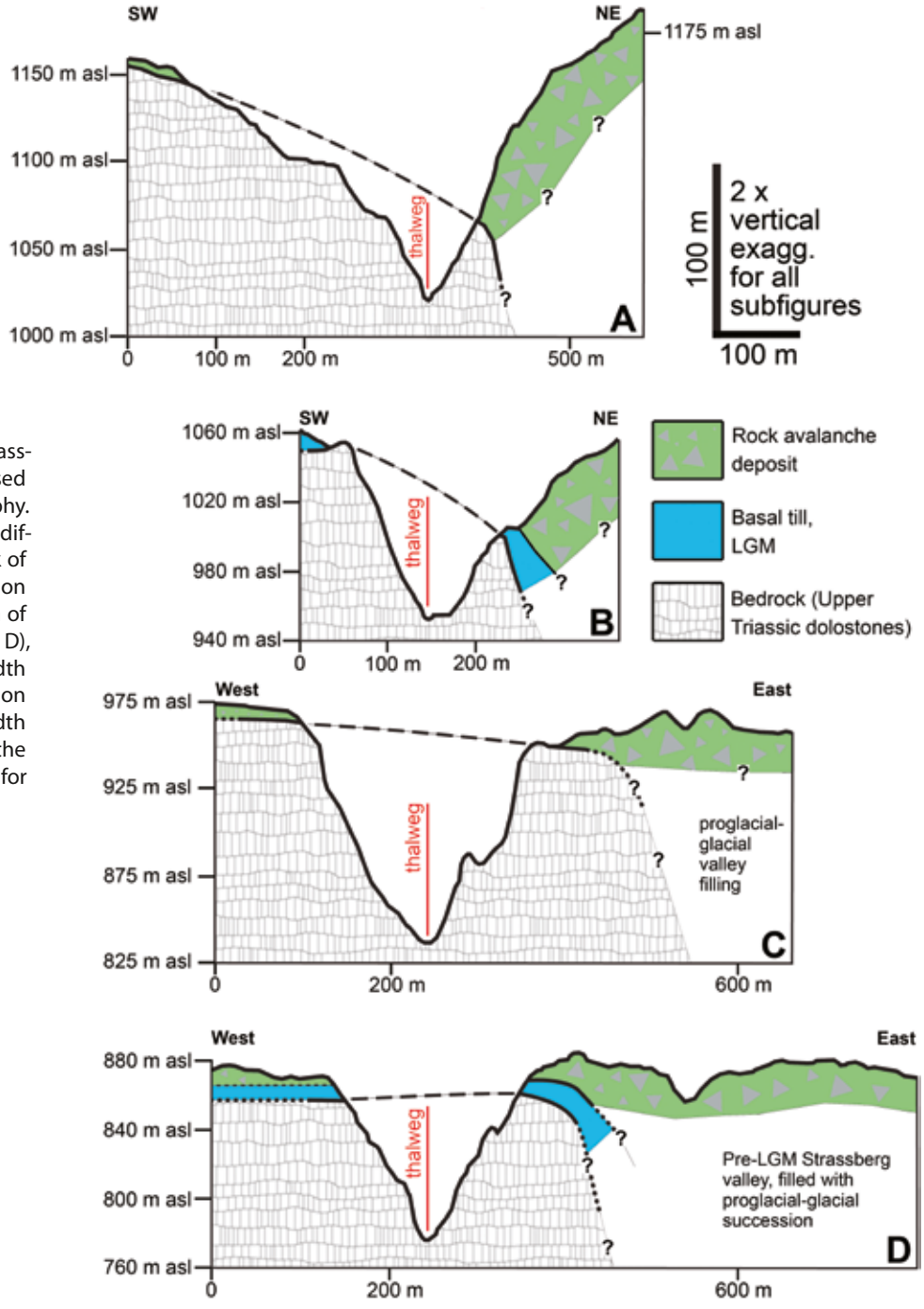

Fig. 10: Cross-sections A to D of Strassberg gorge (see Fig. 1 for position), based on 1-m isohypsed LIDAR topography. Along Strassberg gorge, (a) a marked difference in the altitude of upper brink of bedrock along both valley sides (section A and B), (b) the mapped distribution of Quaternary deposits (section B and D), and (c) an overfit of former valley width filled with Quaternary deposits (section B to D, see also Fig. 1) relative to width of bedrock gorge all suggest that the gorge is post-glacial in age. See text for discussion.

5 Discussion

5.1 22312 rock/snow avalanche

5.1.1 Criteria for identification

On the scree apron of mount Hochwand, after snowmelt, the 22312 deposit might be mistaken for a ‚dry' rockfall. The main criterion against this interpretation is the irregular scatter of boulders downslope and across the apron. If deposited from a dry rockfall, most of the boulders should have ran down to the distal part of the apron, rather than being scattered across large parts of the slope. An exception to this is observed for rockfalls of very small free-fall height or for topplings along the toe of cliffs; in these cases, however, most of the boulders come to rest in the uppermost part of a scree slope very near the cliff toe.

For vertical exposures of fossil talus successions, a similar criterion can be applied. Outsize boulders or clusters of outsize boulders engulfed within the steeply-stratified (30° to >35°) proximal part of fossil talus successions are locally observed. For these situations, several interpretations are possible, all based on field observations: (a) a rockfall boulder bounced down a snow-covered slope, and is readily trapped by the dampening effect of the snow cover high up on the slope (that would be by-passed by the rolling and bouncing boulder if the slope were devoid of snow; (b) the boulder(s) were part of a snow avalanche that not necessarily was triggered by the rockfall that delivered them.

In its present preservation along Alpl valley, the bouldery deposit is readily identified as of rock/snow avalanche origin. If the boulders were part of a cohesive debris flow, they should project from a corresponding deposit (that is not present); if the boulders were carried to site by fluid flow, they should be associated with massive erosional incision and remobilization of older sediment. If the boulders, however, became partly or entirely buried by younger stream-flow and/or debris-flow deposits, their origin from a rockfall-triggered snowflow (=rock/snow avalanche) rather than a debris flow is much less straightforwardly seen.

In deglacial to late-glacial mountain-flank successions, boulders and bouldery deposits are common, but an origin from rock/snow avalanches as transporting agents is only rarely taken into account. In the NCA, late-glacial deposits commonly designated as ‚rockfall moraine' (‚*Bergsturzmoräne*'; in German meaning both the moraine landform and the till) are widespread; under this heading, both, bouldery moraines *s. str*. and lenses and sheets of boulders are subsumed. At least some of these ‚rockfall moraines' indeed may, entirely or in part, represent deposits of rock/snow avalanches. Numerous observations indicate that even highly energetic and destructive ground avalanches (e.g, that breach lanes into forests by uprooting trees) of snow do not mobilize large numbers of boulders; in many cases, simply because there are no larger accumulations of boulders along avalanche tracks. Snowflow deposits laden with numerous boulders thus most probably were triggered by the rockfall that delivered the boulders. In conclusion, only a highly energetic rockfall kicking off and combined with a snow flow can effectively disperse large amounts of clastic material over mountain flanks and valleys, with a mobility and runout commonly ascribed to ‚pure' rock avalanches of much larger volume only.

5.1.2 Two-layer rock/snow avalanche movement

Field evidence shows that the separation into a scree-laden upper layer and a pure-snow lower avalanche layer took place by frontal entrainment of snow in a very early stage of avalanche development (see **Sanders et al., 2014**). The observation that boulders up to 15 m in diameter were rafted projecting atop from the snow indicates that the moving mass had the competence to sustain that weight. The fact that the avalanche deposit shows slide planes merely is an expression of non-turbulent flow in a medium of finite shear strength. Strain localization along shear planes indicates a quasi- laminar flow (at least during the slower phase of avalanche propagation); the slide planes of ice record shear melting. If the water film produced upon shear melting can not escape rapidly enough, fluid pressure (or, in other

terms, the incompressibility of the fluid) would suffice to sustain the boulders weight. Because shear melting is proportional to loading (normal stress) and shear velocity, the water film will adjust in feedback to the weight of the overlying boulder.

The granular snow in itself, however, has a capacity to temporally sustain large weights; otherwise, a snow layer should (physically impossible) instantaneously melt when loaded. Again, it is water films on the surface of the snow grains (cf. **Persson, 2015**) that first provide the contact between the grains; upon loading and pressure melting, if the pore space between grains is occluded by melt-induced strain (as a first reaction to loading), most of the load may be even sustained by suprahydrostatic fluid pressure in occluded grain interstitials. These two mechanisms apply to quasi-laminar snow flow. It is not certain, however, whether coarse-grained snow could sustain a boulder's weight on top if avalanche flow were fully turbulent over a larger distance. Although even in a turbulent snow flow, the permanent building and re-arrangement of grain bridges provides matrix strength against normal (vertical) loads, this is probably not as efficient as the mechanisms in laminar flow.

Water closely approximates a Newtonian fluid, i.e., it has practically no critical shear strength before yield. Thus, the superlong runout of the two-layer scree/snow avalanche is explained by sliding on films of water. From this perspective, one might rather ask why the avalanche stopped at all. We suggest that the stopping resulted from an interplay of: (a) basal friction with snowless ground and asperities along the head of the avalanche, leading to and accompanied by (b) progressive vertical climb (=stacking) and upflow steepening of slide planes, and (c) with progressive slowing of the avalanche, refreezing along slide planes. Finally, when an equilibrium between downslope and upslope forces was attained, the avalanche stopped.

5.2 Old rock avalanche and Strassberg gorge

The old rock avalanche detached from a cliff delimited by a branch of the Telfs fault zone. Along this fault relatively incompetent, backweathering cellular dolomites of the NAR beds are juxtaposed against outweathering, competent Wetterstein Limestone. As mentioned, the Telfs fault zone is seismically active. Macroseismic activity sufficiently intense to cause surface deformation is also suggested by the diverse brittle and soft-sediment deformation structures in the Quaternary talus breccias at Hintereggen. The distribution of rockslides in the Eastern Alps shows that they are closely tied to seismogenic faults, and the Hohe Munde rock avalanche is no exception (**Ostermann & Sanders, 2015**).

West of Strassberg gorge, the presence of large parts of the RAD as a patchy, thin veneer littered with boulders suggests that in this part the avalanche may have propagated over snow. Without a substrate to slide on, the low thickness of the deposit could not have provided the kinematic coupling and kinetic energy required for transport of boulders. This is further supported by the patchiness of deposits. Patchy distribution of clastic sediment is also observed in the distal part of recent rock avalanches over snow.

This interpretation were quite straightforward if the slumpings along that slope are not taken into account. The slumpings affect both the glacial till underneath as well as the overlying RAD. Slumping may be a direct consequence of, or at least might have been initiated by, melting of the hypothetical scree/snow avalanche that deposited the RAD. Alternatively, slumping took place somewhen after and independent of rock avalanching, and led to thinning and patchiness of the deposit. Unfortunately, outcrops are not of sufficient extent and depth to allow for distinction of hypotheses.

As described, the rock avalanche clogged the *upper* part of the old (pre-LGM) Strassberg valley; in the *lower* part of the old Strassberg valley, the rock avalanche propagated over a valley filling of proglacial and glacial deposits. This suggests that the post-LGM clearing of sediments out of and stream re-incision along the old Strassberg valley was still in an initial stage when the rock avalanche descended and clogged the valley. The base-level placed by the rock avalanche controls sediment aggradation in the Strassberg intramontane basin til today. Field mapping provides no evidence that another type of deposit (e.g., till, alluvial fan) except the RAD had set this

base-level. In addition, as a consequence of drainage diversion by rock avalanching, the stream that dewaters the Strassberg catchment incised into the former right-hand bedrock valley flank. The present Strassberg gorge is interpreted to be entirely an epigenetic canyon formed after rock avalanching. The rate of bedrock incision required for canyon formation, of course, depend on the age of the rock avalanche. As mentioned, the highest bulk radiocarbon age from a soil level above the RAD is 11180-11170 cal BP, so the rock avalanche must be older. Within the canyon, the cement of a talus breccia preserved c. 6 m above the present stream thalweg was dated with U/Th to 9 ±1 ka (**Sanders et al., 2010**), so the canyon was incised to this depth at that time. At the exit of Strassberg gorge, the vertical depth of bedrock incision is some 90 m. Assuming that valley incision started at 15 ka, to cut down to the level of the cemented talus breccia, a mean incision rate of 1.5 cm/a over 6 ka is needed. A comparison with rates of bedrock incision deduced for other canyons shows that this is not an outrageously high rate (see **Table 1 in Sanders et al., 2014**), i.e., it is feasible that Strassberg canyon had formed entirely post-glacially in consequence of rock avalanching. In addition, the Hauptdolomit bedrock of the canyon is generally known as an easily erodible lithology. In placing the base-level for the Strassberg basin and its tributaries, blocking the older trunk valley, and causing the incision of the present Strassberg gorge – the rock avalanche exerted a profound and lasting influence on the entire catchment from Telfs up to the apices of scree slopes in Alpl valley.

References

Ampferer, O. & Ohnesorge, T. (1912): Geologische Spezialkarte der im Reichsrate vertretenen Königreiche und Länder der österreichisch-ungarischen Monarchie 1:75.000, 5046 Zirl und Nassereith.– k. k. Geologische Reichsanstalt, Wien.

Collins, G. S. & Melosh, H. J. (2003): Acoustic fluidization and the extraordinary mobility of sturzstroms.– Jour. Geophys Res., 108, B10: 2473, doi:10.1029/2003JB002465.

Crosta, G. B., Chen, H. & Lee, C. F. (2004): Replay of the 1987 Val Pola Landslide, Italian Alps.– Geomorphology, 60: 127-146.

Flatscher, S. (2014): Feinkornverteilungen verschiedener Zerkleinerungsprozesse von Karbonat-Gesteinen.– 83 S., Unpubl. B. Sc. thesis, Univ. of Innsbruck,.

Hungr, O., Morgan, G.C. & Kellerhals, R. (1984): Quantitative analysis of debris torrent hazards for design of remedial measures.– Can. Geotech. Jour., 21: 663-667.

Hungr, O. (1995): A model for the runout analysis of rapid flow slides, debris flows, and avalanches.– Can. Geotech. Jour., 32: 610-623.

McDougall, S. & Hungr, O. (2004): A model for the analysis of rapid landslide motion across three-dimensional terrain.– Can. Geotech. Jour., 41: 1084-1097.

Ostermann, M. & Sanders, D. (2015): Structurally controlled ‚teleconnection' of large-scale mass wasting (Eastern Alps).– Geophys. Res. Abstr., 17: EGU2015-2205-1.

Penck, A. & Brückner, E. (1901/1909): Die Alpen im Eiszeitalter.– 1199 p., Tauchnitz, Leipzig.

Persson, B. N. J. (2015): Ice friction: Role of non-uniform frictional heating and ice premelting.– J. Chem. Phys., 143: 224701, doi: 10.1063/1.4936299.

Poscher, G. (1993): Bemerkenswerte geologische und quartärgeologische Punkte im Oberinntal und dem äusseren Ötztal.– In: Hauser, C. & Nowotny, A. (eds.), Geologie des Oberinntaler Raums, Arbeitstagung 1993, Schwerpunkt Blatt 144 Landeck, 206-219. Geologische Bundesanstalt, Wien.

Preh, A. & Sausgruber, J. T. (2015): The extraordinary rock-snow avalanche of Alpl, Tyrol, Austria. Is it possible to predict the runout by means of single-phase Voellmy- or Coulomb-type models? – In: Lollino, G., Giordan, D., Crosta, G. B., Corominas, J., Azzam, R., Wasowski, J. & Sciarra, N. (eds.): Engineering Geology for Society and Territory–Volume 2. Landslide Processes, 1907-1911, Springer International, Cham.

Preh, A. & Sausgruber J. T. (2016): The rock-snow avalanche of Alpl, Tyrol, Austria. Some considerations regarding the underlying mechanisms. Can. Geotech. Jour., under review.

Prendl, E. (2013): Reproduzierbarkeit von Messungen feinkörniger Karbonat-Sedimente <63 mm mittels Laserdiffraktion.– 49 S., Unpubl. B. Sc. thesis, Univ. of Innsbruck.

Reitner, J. M. (2007): Glacial dynamics at the beginning of Termination I in the Eastern Alps and their stratigraphic implications.– Quat. Int., 164-165: 64-84.

Sanders, D. (2012): Effects of deglacial sedimentation pulse, followed by incision: A case study from a catchment in the Northern Calcareous Alps (Austria).– E&G Quat. Sci. Jour., 61: 16-31.

Sanders, D. (2015): Post-glacial rock avalanche causing epigenetic gorge incision (Strassberg gorge, Eastern Alps).– Geophys. Res. Abstr., 17: EGU2015-2283.

Sanders, D., Ostermann, M. & Kramers, J. (2010): Meteoric diagenesis of Quaternary carbonate-rocky talus slope successions (Northern Calcareous Alps, Austria).– Facies, 56: 27-46.

Sanders, D. & Ostermann, M. (2011): Post-last glacial alluvial fan and talus slope associations (Northern Calcareous Alps, Austria): A proxy for Late Pleistocene to Holocene climate change.– Geomorphology, 131: 85-97.

Sanders, D., Wischounig, L., Gruber, A. & Ostermann, M. (2014): Inner gorge-slot canyon system produced by repeated stream incision (eastern Alps): significance for development of bedrock canyons.– Geomorphology, 214: 465-484.

Sanders. D., Preh, A., Sausgruber, T. (2016): Long-runout rock/snow flows: an underrated type of mass transport and mountain hazard. In: GeoTirol 2016, Annual Meeting DGGV. Geo.Alp, vol. 14, in press.

Senarclens-Grancy, W. (1938): Stadiale Moränen in der Mieminger Kette und im Wetterstein.– Jb. Geol. Bundesanst., 88: 1-12.

Spreafico, M., Lehmann, C. & Naef, O. (1996): Empfehlung zur Abschätzung von Feststofffrachten in Wildbächen. Teil 2: Fachliche Grundlagen und Fallbespiele.– Arbeitsgruppe für operationelle Hydrologie GHO, Mitteilungen Nr. 4, Bern.

Tollmann, A. (1976): Analyse des klassischen nordalpinen Mesozoikums. 580 pp., Franz Deuticke, Wien.

van Husen, D., Reitner, J. (2011): An outline of the Quaternary stratigraphy of Austria. E&G Quat. Sci. Jour., 60: 366-387.

Voellmy, A. (1955): Über die Zerstörungskraft von Lawinen. Schweizerische Bauzeitung 73, 159-165, 212-217, 246-249, 280-285.